

Magnetic loading of magnetars' flares

Maxim Lyutikov [®]★

Department of Physics and Astronomy, Purdue University, 525 Northwestern Avenue, West Lafayette, IN 47907-2036, USA

Accepted 2021 October 26. Received 2021 October 26; in original form 2021 September 6

ABSTRACT

Magnetars, the likely sources of fast radio bursts, produce both steady highly relativistic magnetized winds and occasional ejection events. We demonstrate that the requirement of conservation of the magnetic flux dominates the overall dynamics of magnetic explosions. This is missed in conventional hydrodynamic models of the ejections as expanding shell with parametrically added magnetic field, as well as one-dimensional models of magnetic disturbances. Magnetic explosions from magnetars come into force balance with the pre-flare wind close to the light cylinder. They are then advected quietly with the wind or propagate as electromagnetic disturbances. No powerful shock waves are generated in the wind.

Key words: magnetic fields – pulsars: general – stars: winds, outflows.

1 INTRODUCTION

Observations of correlated radio and X-ray bursts (Bochenek et al. 2020; CHIME/FRB Collaboration 2020; Mereghetti et al. 2020; Li et al. 2021; Ridnaia et al. 2021) established the fast radio burst (FRB)—magnetar connection.

Two kinds of models of FRBs' *loci* are competing at the moment. The first advocates that FRBs are magnetospheric events, e.g. solar flare-like (Lyutikov 2002b, 2006a,c; Lyubarsky 2020; Lyutikov & Popov 2020); the emission mechanism remains unidentified, akin to the 50+ yr problem of pulsar radio emission (see Lyubarsky 2020; Lyutikov 2021, for new ideas). Second are wind-generated GRB-like events (Lyubarsky 2014; Beloborodov 2017, 2020; Metzger, Berger & Margalit 2017; Metzger, Margalit & Sironi 2019; Khangulyan, Barkov & Popov 2021). Emission mechanism is the cyclotron maser (Gallant & Arons 1994; Plotnikov & Sironi 2019; Babul & Sironi 2020). [For discussion of general constraints on plasma parameters and models, see e.g. Lyutikov & Rafat (2019) and Lyubarsky (2021).]

In this paper, we argue that wind models of FRBs are internally inconsistent. Qualitatively, these models use the hydrodynamic paradigm of the internal shock models of GRBs, the flying shells (Piran 2004), with parametrically added magnetic field component. This simple addition of magnetic field cannot be applied in principle to the magnetic explosions of magnetars. The key point is the conservation of the magnetic flux within the exploding plasma. This is related to the sigma problem in pulsar winds (Rees & Gunn 1974; Kennel & Coroniti 1984), reformulated by Blandford (2002) as a magnetic flux conservation problem (see also Lyutikov & Blandford 2003; Lyutikov 2006b). The theoretical difference between the two models (the 'magnetized shells' and the present model) is enormous. Instead of highly relativistic shock with the Lorentz factor over a million, as advocated by e.g. Beloborodov (2020), the magnetic explosion comes into a force balance approximately near the light cylinder, and propagates as an electromagnetic (EM) pulse there on.

We first give an analysis of the wind-FRB models (Metzger et al. 2019; Beloborodov 2020) from the point of basic theory of pulsar winds and relativistic shock propagating through the winds (Section 2). These are the types of 'double relativistic explosion' previously considered in various set-ups by Lyutikov (2002a, 2011, 2017), Lyutikov & Camilo Jaramillo (2017), and Barkov, Luo & Lyutikov (2021). In Section 3, we argue that an effective 'magnetic loading' quickly reduces the power of the magnetar's explosion, producing either an EM pulse through the wind or a confined magnetic structure in pressure balance with the wind. No ultra-relativistic shocks are produced.

2 THE PULSAR WIND AND SHOCK DYNAMICS IN THE MAGNETIZED WIND

2.1 Pulsar wind primer

Pulsar and magnetars produce relativistic highly magnetized winds (Michel 1969, 1973; Goldreich & Julian 1970), which can be parametrized by the wind luminosity $L_{\rm w}$ and the ratio of Poynting to particle fluxes:

$$\mu_{\rm w} = \frac{L_{\rm w}}{\dot{N}m_{\rm e}c^2} = \frac{B_{\rm LC}^2}{4\pi n_{\rm LC}m_{\rm e}c^2},\tag{1}$$

where \dot{N} is the rate of lepton ejection by the neutron star; subscript LC indicates values measured at the light cylinder, and

$$R_{\rm LC} = 4 \times 10^9 P \text{ cm} \tag{2}$$

for the period of a star P measured in seconds. Expected values of $\mu_{\rm w}$ are in the range of 10^4 – 10^6 (Arons & Scharlemann 1979; Arons 1983; Hibschman & Arons 2001; Beloborodov & Thompson 2007). In the case of GJ scaling of density, with multiplicity $\kappa = n/n_{\rm GJ}$,

$$\dot{N} = \kappa \frac{\sqrt{cL_{\rm w}}}{e}.\tag{3}$$

No powerful shocks are generated. Hence, there is no emission of FRBs from the far wind.

^{*} E-mail: lyutikov@purdue.edu

Initially, the wind accelerates linearly away from the light cylinder

$$\Gamma_{\rm w} = \frac{r}{R_{\rm LC}} \tag{4}$$

so that the wind magnetization decreases

$$n' = \left(\frac{R_{\rm LC}}{r}\right)^{-3} n_{\rm LC},$$

$$B' = \left(\frac{R_{\rm LC}}{r}\right)^{-2} B_{\rm LC},$$

$$\sigma(r) = \frac{B'^{2}}{4\pi n' m_{\rm e} c^{2}} = \frac{R_{\rm LC}}{r} \mu_{\rm w},$$
(5)

where primes denote quantities measured in the wind frame.¹

The terminal value for the wind acceleration is the Alfvén condition.

$$\Gamma_{\rm w} = \sigma_{\rm w}^{1/2} = \mu_{\rm w}^{1/3}$$
 $\sigma_{\rm w} = \mu_{\rm w}^{2/3} \gg 1$ (6)

reached at

$$R_{\rm w} = \mu_{\rm w}^{1/3} R_{\rm LC} = \Gamma_{\rm w} R_{\rm LC}. \tag{7}$$

Total energy and mass (in lab frame) contained in the acceleration region,

$$E_{\rm w} = L_{\rm w} \frac{R_{\rm w}}{c}$$

$$M_{\rm w} = m_{\rm e} \dot{N} \frac{R_{\rm w}}{c}, \tag{8}$$

are typically insignificant; mass loading of the following shock is further reduced by $1/\Gamma_{\rm w}$.

At distances $r > R_{\rm w}$,

$$\Gamma_{\rm w} = \mu_{\rm w}^{1/3}$$

$$n' = \mu^{-1/3} \left(\frac{R_{\rm LC}}{r}\right)^{-2} n_{\rm LC}$$

$$B' = \mu^{-1/3} \left(\frac{R_{\rm LC}}{r}\right)^{-1} B_{\rm LC}$$

$$\sigma_{\rm w} = \mu_{\rm w}^{2/3}$$

$$\Gamma^* = 2\sqrt{\sigma_{\rm w}} \Gamma_{\rm w} = 2\mu_{\rm w}^{2/3} = 2\Gamma_{\rm w}^2.$$
(9)

Quantity Γ^* is the Lorentz factor (measured in lab frame) required to produce a shock in the receding wind.

The above considerations assume no magnetic dissipation. At the basic level, it is not consistent with observations of the Pulsar Wind Nebulae (PNWe). As Rees & Gunn (1974) and Kennel & Coroniti (1984) argued, σ_w cannot remain $\gg 1$ until the (conventional magnetohydrodynamic, MHD) wind termination shock. It should drop to $\leq 10^{-2}$. This can happen either close to the LC (Coroniti 1990; Lyubarsky & Kirk 2001) or at the termination shock (Lyubarsky 2003; Sironi & Spitkovsky 2009, 2011). As Porth, Komissarov & Keppens (2014) argued, magnetic dissipation can occur in the bulk of the nebula (Porth et al. 2017); still observations of the Crab's inner knot require that a large sector of the wind has low magnetization (Lyutikov, Komissarov & Porth 2016). In the limit of dominant dissipation in the near wind, $\sigma_w \leq 1$, all of spin-down is carried by particle flow; hence, in that case $\Gamma_w = \mu_w \sim 10^4 - 10^6$.

2.2 Explosions in relativistic winds

Let us next consider explosions in the preceding magnetar wind. We assume that some kind of the central engine (a magnetar) produces energetic events on top of the steady wind. This will constitute a type of double relativistic explosion (Lyutikov 2002a, 2011, 2017; Lyutikov & Camilo Jaramillo 2017; Barkov et al. 2021). First, we solve a formal MHD problem, and then discuss its limitations.

2.2.1 Point explosion in relativistic fluid wind

Consider a relativistic fluid wind of luminosity L_w moving with Lorentz factor Γ_w :

$$L_{\rm w} = 4\pi r^2 \Gamma_{\rm w}^2 m_{\rm w}' m_{\rm e} c^3 = \Gamma_{\rm w} \dot{M}_{\rm w} c^2, \tag{10}$$

where $n'_{\rm w}$ is the density in the wind frame; the lab frame density is $n_{\rm w} = \Gamma_{\rm w} n'_{\rm w}$.

Consider an explosion that involves energy $E_{\rm ej}$ and no mass $M_{\rm ej}=0$. Thus, we assume that the energy of the explosion is transferred to the wind instantaneously. Consider a shock moving with Lorentz factor $\Gamma\gg\Gamma_{\rm w}$ (as measured in lab frame). In a shock frame, typical energy of post-shock particles is $T_2\sim\Gamma/(2\Gamma_{\rm w})$. The shock sweeps particles, giving them bulk Lorentz factor Γ ; at radius r, the swept-up mass (in lab frame) is $L_{\rm w} r/(c^2\Gamma_{\rm w})$. Thus,

$$\Gamma \sim \sqrt{2}\Gamma_{\rm w}\sqrt{\frac{R_0}{r}},$$
(11)

where

$$R_0 = \frac{c E_{\rm ej}}{L_{\rm w}}.\tag{12}$$

2.2.2 Point explosion in relativistic magnetized wind

Relativistic explosions in static magnetic configurations were studied by Lyutikov (2002a), producing self-similar solutions of the kind of Blandford & McKee (1976). Let us generalize them to the moving media. Below, we are not interested in the structure of the flow (it will be the same as found in Lyutikov 2002a), but in the overall scaling of the shock Lorentz factor Γ dependence on the wind parameters.

Let us first consider a simple, extreme case of point magnetospheric explosion with no mass loading. Let the wind preceding the ejection have magnetization $\sigma_w \gg 1$. Neglecting small contribution to the wind luminosity from the particles,

$$L_{\rm w} = 4\pi r^2 \Gamma_{\rm w}^2 \frac{B_{\rm w}^{\prime,2}}{4\pi} c. \tag{13}$$

Consider again an explosion that involves energy $E_{\rm ej}$ and no mass $M_{\rm ej}=0$. The interaction in the accelerating region $r \leq R_{\rm w}$, before the wind reaches $\Gamma_{\rm w}$, does not affect much the flow, because of small $E_{\rm w}$ and $M_{\rm w}$, high values of $\sigma(r)$, and the fact that both the ejecta and the wind accelerate linearly with r. (This statement has been verified according to the following discussion.)

Consider a shock moving with Lorentz factor Γ (as measured in lab frame) through a highly magnetized wind, which itself is moving with Γ_w . Let the values of the magnetic field in the lab frame before the shock be B_w ,

$$B_{\rm w} = \frac{\sqrt{L_{\rm w}}}{\sqrt{r}c}$$

$$B'_{\rm w} = \frac{B_{\rm w}}{\Gamma_{\rm w}}$$
(14)

¹This definition of magnetization parameter $\sigma_{\rm w}$ is relevant only at $r\gg R_{\rm LC}$ as it does not take into the account large parallel momenta of particles near the light cylinder.

(prime is in wind frame). The shock is moving through the wind with

$$\Gamma_{\rm s} = \frac{\Gamma}{2\Gamma_{\rm cr}}.\tag{15}$$

In the frame of the shock, the shocked part of the wind moves with Lorentz factor $\sqrt{\sigma_w}$. It carries magnetic field

$$B_2' = \frac{\Gamma}{2\Gamma_{\rm w}\sqrt{\sigma_{\rm w}}} B_{\rm w}' \tag{16}$$

as measured in the post-shock frame. The post-shock frame moves with Lorentz factor $\Gamma/(2\sqrt{\sigma_w})$ in lab frame; thus,

$$B_{\rm w,2} = \left(\frac{\Gamma}{\Gamma^*}\right)^2 B_{\rm w}.\tag{17}$$

This is magnetic field in the post-shock region as measured in the lab frame.

The swept-up material is located within

$$\Delta r \sim \frac{\sigma}{\Gamma^2} r.$$
 (18)

The energy budget reads (particle contribution is neglected for $\sigma_{\rm w} \gg 1$)

$$E_{\rm ej} = c \left(B_{\rm w,2}^2 \right) r^2 \Delta r \approx L_{\rm w} r \frac{\Gamma^2}{4\sigma_{\rm w} \Gamma_{\rm w}^4}. \tag{19}$$

Thus.

$$\Gamma = 2\Gamma_{\rm w}^2 \sqrt{\sigma_{\rm w}} \sqrt{\frac{R_0}{r}} \to 2\sqrt{\frac{R_0}{r}} \Gamma_{\rm w}^3, \tag{20}$$

where the last relation assumed $\Gamma_{\rm w} = \sqrt{\sigma_{\rm w}}$. Notice the difference in the power of $\Gamma_{\rm w}$ in comparison with the fluid case (11).

In observer time,

$$t_{\rm ob} = \frac{t}{2\Gamma^2} = \frac{ct^2}{8R_0\Gamma_{\rm w}^4\sigma_{\rm w}}$$
$$\Gamma = 2^{1/4}\Gamma_{\rm w}\sigma_{\rm w}^{1/4} \left(\frac{R_0}{ct_{\star}}\right)^{1/4}.$$
 (21)

The energy is concentrated in

$$\frac{\Delta r}{r} = \frac{1}{8\Gamma_{\rm w}^4} \frac{r}{R_0} \tag{22}$$

(independent of $\sigma_{\rm w}$).

2.3 Shock interaction of relativistic winds

Let's next assume that the first wind is followed by the second wind from the flare with Lorentz factor Γ_f , wind frame magnetic field B_f , and magnetization σ_f :

$$L_f = \Gamma_f^2 B_f^2 r^2 c. \tag{23}$$

We assume strong interaction, so that a reverse shock (RS) is generated in the flare wind and forward shock (FS) is generated in pre-explosion wind. Let in the lab frame the contact discontinuity between two winds move with Lorentz factor Γ_{CD} . Then,

$$\Gamma_{\rm FS} = 2\sqrt{\sigma_{\rm w}}\Gamma_{\rm CD}$$

$$\Gamma_{\rm RS} = \frac{\Gamma_{\rm CD}}{2\sqrt{\sigma_{\rm f}}}.$$
(24)

Lorentz factor of the RS with respect to the flare flow is

$$\Gamma_{RS}' = \frac{\Gamma_{f}}{\Gamma_{CD} \sqrt{\sigma_{f}}}.$$
 (25)

Balancing magnetic field in the shocked wind and shocked flare

$$\frac{\Gamma_{\rm CD}}{\Gamma_{\rm w}^2} \frac{\sqrt{L_{\rm w}}}{\sqrt{c}r} = \frac{1}{2\Gamma_{\rm CD}} \frac{\sqrt{L_{\rm f}}}{\sqrt{c}r},\tag{26}$$

we find that

$$\Gamma_{\rm CD} = \left(\frac{L_{\rm f}}{L_{\rm w}}\right)^{1/4} \Gamma_{\rm w},$$

$$\Gamma_{\rm FS} = 2 \left(\frac{L_{\rm f}}{L_{\rm w}}\right)^{1/4} \Gamma_{\rm w} \sqrt{\sigma_{\rm w}},$$

$$\Gamma_{\rm RS} = \frac{1}{2} \left(\frac{L_{\rm f}}{L_{\rm w}}\right)^{1/4} \frac{\Gamma_{\rm w}}{\sqrt{\sigma_{\rm f}}},$$

$$\Gamma'_{\rm RS} = \left(\frac{L_{\rm f}}{L_{\rm w}}\right)^{1/4} \frac{\Gamma_{\rm f} \sqrt{\sigma_{\rm f}}}{\Gamma_{\rm w}}.$$
(27)

Strong shock conditions require that post-shock temperatures are relativistic. For the FS,

$$T_{\text{FS}} = \frac{1}{8\sqrt{\sigma_{\text{w}}}} \frac{\Gamma_{\text{FS}}}{2\Gamma_{\text{w}}} > 1 \rightarrow \frac{1}{8} \left(\frac{L_{\text{f}}}{L_{\text{w}}}\right)^{1/4},$$

$$L_{\text{f}} \geq 4 \times 10^{3} L_{\text{w}}.$$
(28)

For the RS.

$$T_{RS} = \frac{1}{8} \left(\frac{L_{f}}{L_{w}}\right)^{1/4} \frac{\Gamma_{f}}{\Gamma_{w}},$$

$$\Gamma_{f} \ge 8 \left(\frac{L_{f}}{L_{w}}\right)^{1/4} \Gamma_{w}.$$
(29)

Curiously, the fraction of the flare wind η_{RS} used to push the magnetar wind increases with its magnetization:

$$\eta_{\rm RS} \sim \frac{1}{\Gamma_{\rm RS}^2} = 4 \left(\frac{L_{\rm w}}{L_{\rm f}}\right)^{1/2} \frac{\sigma_{\rm f}}{\Gamma_{\rm w}^2}.$$
(30)

This is because for higher σ_f the RS moves faster through the flare wind $[\eta_R]$ is not the dissipated power that is put into particles, that one is smaller by $\Gamma'_{RS}/(8\sqrt{\sigma_f})]$.

The main constraint for the wind-wind interaction comes from the fact that the flare wind should be supersonic with respect to the magnetar wind. To make a shock in the preceding wind, it is required that

$$\Gamma_{\rm f} > \Gamma^* = 2\Gamma_{\rm w} \sqrt{\sigma_{\rm w}} = 2\Gamma_{\rm w}^2. \tag{31}$$

Since acceleration of the flare proceeds according to the same law (7), this requires

$$\Gamma_{\rm f} = \sqrt{\sigma_{\rm f}},$$

$$\sigma_{\rm f} \ge 4\Gamma_{\rm w}^4.$$
(32)

Since terminal magnetization is related to the parameter μ_w by (9), it is required that

$$\mu_{\rm f} = \sigma_{\rm f}^{3/2} = 8\Gamma_{\rm w}^6. \tag{33}$$

Thus, the flare wind must be much cleaner than the initial wind

$$\frac{\mu_{\rm f}}{\mu_{\rm w}} > 8\Gamma_{\rm w}^4. \tag{34}$$

2.4 The fluid engine

Earlier, we took an extreme position, that the energy transfer from the ejecta to the wind was instantaneous, zero mass and zero magnetic loading at the explosion site. In fact, energy transfer between two

2692 M. Lyutikov

relativistically expanding and relativistically accelerating flows will be inefficient. Two factors are at play. First, there is a problem with creation of shocks during the acceleration stage of the wind: In the acceleration region, the magnetization is extremely high (equation 5). It is very hard to create a shock in a highly magnetized flow. Consider for example a fluid explosion starting with ejection at $R_{\rm ej} \leq R_{\rm LC}$. Acceleration of the fluid ejecta is linear at first (Paczynski 1986)

$$\Gamma_{\rm ej} = \frac{r}{R_{\rm ej}}.\tag{35}$$

At the wind acceleration stage $r < R_w$, the condition that the ejecta makes a strong shock in the preceding wind is (see equation 5)

$$\Gamma_{\rm ej} \ge 2\sqrt{\sigma(r)}\Gamma(r) = 2\mu_{\rm w}^{1/2}\sqrt{\frac{r}{r_{\rm LC}}}.$$
 (36)

This requires

$$\frac{r}{R_{\rm LC}} \ge (256\mu_{\rm w}) \left(\frac{R_{\rm ej}}{R_{\rm LC}}\right)^2. \tag{37}$$

Since $\mu \gg 1$, the fluid ejecta just starts to make a shock at large distances.

Secondly, shock or not, if there is an overpressurized region with energy density u in the lab frame, which is expanding with Lorentz factor Γ , then the energy density in the frame associated with the interface of the two interacting media is $\sim u/\Gamma^2$. This is the force per unit area that contributes to the acceleration of a lower pressure region. The acceleration time (energy transfer time) in the lab frame $t_{\rm acc}$ is slower by another factor of Γ ; hence, the shortest time to transfer energy from the ejecta to the previous wind is $t_{\rm acc} \sim \Gamma^3(r/c)$. For example, if interaction starts at $R_{\rm w} \sim \Gamma_{\rm w} R_{\rm LC}$ (7), the energy transfer time is $\sim \Gamma_{\rm w}^4 R_{\rm LC}$.

3 MAGNETICALLY DRIVEN EXPLOSIONS

3.1 Not 'magnetic shells'

Earlier, we summarized the dynamics of magnetized shocks in magnetized winds. We did not address in detail the energy release process; we just highlighted in Section 2.4 possible issues with the fluid engine. The early dynamics is the key. As we are interested in magnetic explosions from highly magnetized magnetar, both the engine and the explosion are magnetic.

Typically, magnetic explosions were considered in a framework of the internal shock model of GRB (Piran 2004), as analogue of flying fluid shells (e.g. Beloborodov 2020), but with internal magnetic field. This is not correct in principle: Dynamics of magnetic explosions cannot be reduced to 'magnetized shells'.

First, in the case of one-dimensional (1D) magnetic explosion Lyutikov (2010) found a fully analytical 1D solution, a simple wave, for a non-stationary expansion of highly magnetized plasma into vacuum and/or low-density medium. The result is somewhat surprising: Initially, the plasma accelerates as $\Gamma \propto t^{1/3}$ and can reach terminal Lorentz factor $\Gamma_f = 1 + 2\mu_0$, where μ_0 is the initial magnetization (see also Levinson 2010). Thus, it was shown that time-dependent explosions can achieve much larger Lorentz factors than the steady-state flows: $2\mu_0$ for non-steady state versus $\mu_0^{1/3}$ for steady state (in this particular application, $\mu_0 = \sigma_0$). The force-free solution was generalized to the MHD regime (using a mathematically tricky hodograph transformation by Lyutikov & Hadden 2012).

Importantly, those were specifically 1D models of local breakout of magnetized jet from, e.g. a confining star in GRB outflows. They cannot be simply used to describe fully three-dimensional

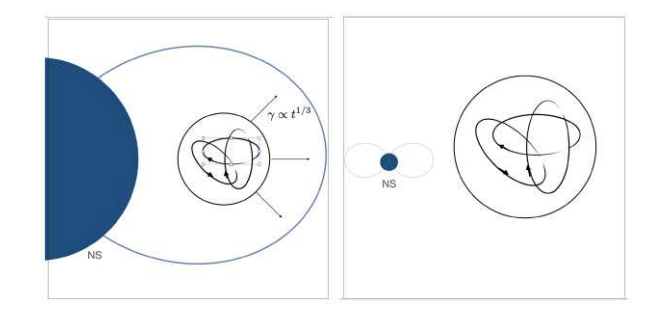


Figure 1. Cartoon of magnetic explosion. Left-hand panel: a solar flare-type event near the surface of the neutron star produces a magnetically disconnected magnetized cloud with complicated (linked) internal magnetic structure and total internal pressure (magnetic field and pairs) slightly exceeding the local dipole field. As the magnetic blob expands, its pressure quickly becomes larger than that of the surrounding dipolar one. Expansion quickly becomes relativistic. Later on, as the blob expands, magnetic field in the blob scales as $B_{\rm b} \sim 1/R^2$, much faster than the magnetic field in the wind. As a result, the expelled blob quickly reaches pressure equipartition with the wind flow.

magnetic explosions. What is different in multidimensional magnetic explosions is the conservation of the magnetic flux. Such issues do not appear for 1D motion.

As Rees & Gunn (1974) and Kennel & Coroniti (1984) argued, the presence of the global magnetic field changes the dynamics completely if compared with the fluid case. Lyutikov & Blandford (2003) and Lyutikov (2006b) reformulated the problem in terms of the magnetic flux: The σ problem is the problem of the (properly defined) toroidal magnetic flux conservation. Below, we apply those ideas to the launching region of magnetic explosions.

3.2 Dynamics of magnetic explosion

Let's assume that a magnetospheric process (e.g. flare-like event) created a magnetic bubble, disconnected from the rest of the magnetosphere. The bubble contains both toroidal and poloidal magnetic fluxes (Fig. 1).

The strong gradient of the dipolar field will push the magnetic bubble away. It will quickly become highly overpressurized, and will start expanding. The expansion will have two stages. First, near the surface of the bubble the field is purely tangential. At this stage, expansion is described by the 1D model of Lyutikov (2010). If initial magnetization within the bubble was σ_0 , the flow becomes supersonic at the moment the expansion reaches $\Gamma = (\sigma_0/2)^{1/3}$. Unlike the stationary wind when acceleration ends at the sonic point, non-stationary magnetic explosion continues to accelerate to $\Gamma = 1 + 2\sigma_0$.

After a rarefaction wave propagated deep inside the magnetic bubble, the expansion dynamics changes. The bubble consists of closed magnetic loops. Flux conservation requires that the magnetic field with the bubble scales as $B \propto 1/R^2$, where R is a current size of the bubble. As long as the expelled blob is inside the light cylinder, the dipolar field decays much faster $\propto 1/R^3$ (the bubble is also moving away from the star, so it is located approximately at a distance R comparable to its size), so the expansion of the blob occurs almost like in vacuum. The energy contained within a blob decreases $E \sim B^2 R^4 \propto R^{-1}$. When the size of the expanding bubble becomes larger than the light cylinder, the external magnetic field changes its scaling from $\propto R^{-3}$ to $\propto R^{-1}$. Thus, the bubble quickly reaches equipartition with the wind field.

For example, if the bubble is created near the neutron star with typical energy

$$E_{\rm f} \sim B_{\rm f}^2 R_{\rm f}^3. \tag{38}$$

The magnetic field inside the newly created magnetic cloud is of the order of the NS's surface field $B_{\rm NS}$, $B_{\rm f} \sim B_{\rm NS}$, and a size smaller than $R_{\rm NS}$, $R_{\rm f} = \eta_R R_{\rm NS}$, $\eta_R \ll 1$. (Only giant flares need $\eta_R \sim 1$; FRBs with nearly quantum magnetic field need about a football field of energy to account for the high-energy emission, $\eta_R \sim 10^{-2}$; see Section 3.5.) So

$$E_{\rm f} \sim \eta_{\rm R}^3 B_{\rm NS}^2 R_{\rm NS}^3. \tag{39}$$

Given the $\propto 1/R^2$ decrease of the magnetic field within the bubble, the pressure balance between the expanding flux tube and the wind at $r \ge R_{\rm LC}$ gives the radius $R_{\rm eq}$ when the expanding flux tube reaches the force balance with the wind

$$\frac{R_{\rm eq}}{R_{\rm LC}} = \eta_R^{3/2} \frac{R_{\rm LC}}{R_{\rm NS}}.$$
 (40)

Since $\eta_R \ll 1$, this is achieved fairly close to the light cylinder.

At larger distances, the bubble is just advected with the wind, always kept at the force balance on the surface. The light bubble is also first accelerated with the wind, and then coasts (at $r > R_{\rm w}$). Since in the coasting stage the confining magnetic field decreases as 1/r, the size of the bubble increases as $R_{\rm bubble} \propto r^{1/2}$. Eventually, when the magnetar's wind starts interacting with the interstellar medium (ISM), the ejected bubble shocks the ISM and produces radio afterglow (Cameron et al. 2005; Gaensler et al. 2005) seen after the giant flare of SGR 1806–20 (Hurley et al. 2005; Palmer et al. 2005), as described by Mehta, Barkov & Lyutikov (2021).

3.3 Where did all the energy go? – magnetic loading

We seem to run into a little paradox. In the case of FRBs, the newly created magnetic bubble with energy (39) would have more energy than the energy of the magnetic field measured at the light cylinder, within the volume of a light cylinder,

$$E_{\rm f} \gg E_{\rm LC} \sim \frac{B_{\rm NS}^2 R_{\rm NS}^6}{R_{\rm LC}^3}.$$
 (41)

Yet, the expanding bubble came into force balance with the preceding wind near the light cylinder. Where did the extra energy go?

It went into the stretching of the internal magnetic field of the bubble. Recall that the pressure of the magnetic field along the field is negative: The field 'wants' to contract. Stretching the field (expanding loops of the tangled magnetic field) requires work to be done against the contracting parallel force. The overpressurized magnetically dominated configuration 'forces' the field to expand, thus making work on the internal field. As a result, most of the excess magnetic energy is spent on stretching the internal magnetic field, not on producing shocks/making pdV work on the surrounding medium. This effect can be called as magnetic loading.

We come to an important conclusion: Magnetic explosions are dominated not by the mass loading, but by the magnetic loading. Even very powerful explosion, with energies much larger than $B_{\rm LC}^2 R_{\rm LC}^3$, reaches a force balance close to the light cylinder. After that, they are locked in the flow, and quietly advected.

3.4 Expanding spheromak/flux ropes

To illustrate the above points, one can assume that a newly created bubble resembles a spheromak (Bellan 2000). A possible model

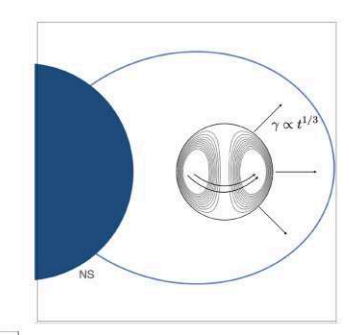




Figure 2. Cartoon of magnetic explosion of a spheromak. Left-hand panel: a solar flare-type event near the surface of the neutron star produces a magnetically disconnected magnetized cloud, a spheromak. Expansion is mostly equatorial. Right-hand panel: during further expansion, the magnetic flux in the tube remains constant. As a result, the tube quickly reaches the force balance with the wind. After that, the flux tube forms a conically expanding structure

of the newly created magnetic cloud is a slightly overpressured spheromak (Fig. 2). We can appeal then to the fully analytical solution for non-relativistically expanding spheromak (Lyutikov & Gourgouliatos 2011). The total magnetic helicity, as well as the toroidal magnetic flux, is constant, while $B \propto 1/R^2$. Also, for a particular case of expansion with velocity r/(ct) the corresponding solutions are fully relativistic (Prendergast 2005; Gourgouliatos & Lynden-Bell 2008). The total energy of the expanding spheromak

$$E_{\rm tot} = \int dV \frac{E^2 + B^2}{8\pi} \propto \frac{B_0^2 R_0^4}{R}$$
 (42)

decreases. These are a fully analytical solution illustrating the principal points made in Section 3.2.

The late expansion of a spheromak will be somewhat different though. On the surface, the magnetic field of the spheromak scales as $B_{\perp} \propto \sin \theta$. Thus, initial expansion will be mostly equatorial. The expanding part of the spheromak, with high toroidal magnetic field, becomes causally disconnected and forms an expanding magnetic flux tube, right-hand panel in Fig. 2 [Lyutikov & Gourgouliatos (2011) also discussed the expanding flux rope, though in that case the solution is approximate].

Some difference in evolution between an expanding bubble and a flux tube appears after they reached force balance with the wind. In case of the flux tube, consider a magnetic flux tube initially containing magnetic field B, overall radius R, and cross-section S (Fig. 2). The conservation of the magnetic flux requires BS = constant. Thus, as the flux tube inflates its energy E_B evolves according to

$$E_B = \frac{R}{R_0} \frac{S_0}{S} E_{B,0}. \tag{43}$$

If the external magnetic field scales as $\propto R^{-\alpha}$, then the cross-section evolves as

$$S = \left(\frac{R}{R_0}\right)^{\alpha} S_0. \tag{44}$$

If a flux tube occupies a polar angle $(\Delta \theta)$ and has radial extent (Δr) ,

$$\frac{(\Delta r)(\Delta \theta)}{(\Delta r)_0(\Delta \theta)_0} = \left(\frac{R}{R_0}\right)^{\alpha - 1}.$$
 (45)

Thus, in a wind $\alpha = 1$, $(\Delta r)(\Delta \theta)$ = constant: The flux tube expands along conical surface with constant thickness.

Thus, after reaching a force balance close to the light cylinder the ejected flux tube remains in force balance with the wind. The energy contained in the flux tube remains constant: Expanding magnetic flux tube does not do any work on the surrounding.

In passing, we note that both spheromaks and flux tube models were discussed for solar CME (Farrugia, Osherovich & Burlaga 1995).

3.5 Applications to SGR 1935+2154 X-ray/radio flares

In the case of SGR 1935+2154, Burst-G, unambiguously associated with radio pulse (Mereghetti et al. 2020), had a peak X-ray luminosity of $\sim \! 10^{40}$ erg s $^{-1}$ and total released energy $E_{\rm f} \sim 10^{39}$ erg. The G burst was also particularly spectrally hard. The accompanying radio burst had 3 \times 10 34 erg; the radio to high energy fluence was $F_{\rm R}/F_{\rm X} \sim 2 \times 10^{-5}$. The period is 3.4 s (so $R_{\rm LC} = 1.4 \times 10^{10}$ cm, $R_{\rm LC}/R_{\rm NS} = 1.4 \times 10^4$). The spin-down luminosity is 1.7 \times 10 34 erg s $^{-1}$ and the surface magnetic field is $B_{\rm NS} = 2.2 \times 10^{14}$ G (Israel et al. 2016).

Since the process of launching of any outflow is energetically the most demanding step, and assuming that an approximately half of the energy was dissipated, we estimate the ejection energy as the energy of the X-ray burst. The required volume of the magnetosphere that got dissipated to power the X-ray flare is

$$R_{\rm f} \sim \frac{E_{\rm f}^{1/3}}{B_{\rm NS}^{2/3}} = 3 \times 10^3 \,{\rm cm},$$

 $\eta_R = \frac{R_{\rm f}}{R_{\rm NS}} = 2 \times 10^{-3}.$ (46)

A flare was just only 30 m in size.

Expected wind coasting radius (7) is $R_{\rm w} = 1.7 \times 10^{12} (\Gamma_w/100)$ cm; scale (12) is $R_0 = 1.7 \times 10^{15}$ cm.

The flare released energy much larger than the magnetic energy at the light cylinder:

$$\frac{E_{\rm f}}{E_{\rm LC}} = 6 \times 10^4. \tag{47}$$

The equipartition radius (40) evaluates to

$$\frac{R_{\rm eq}}{R_{\rm LC}} = 2. \tag{48}$$

Thus, the expanding blob reached equipartition right near the light cylinder, consistent with our conclusion on the general FRB population.

4 DISCUSSION

We demonstrate that the wind models of FRBs are internally inconsistent on several grounds. The wind-type models of FRBs had a clear 'good' point: *If* (only *if*!) one can make a relativistic shock in a relativistically receding wind, the combined Lorentz factor of the shock and (two times) the wind's Lorentz factor make for an

extremely high Lorentz factor shock, hence short durations from large distances.

There are serious problems with this scenario. First, regardless of the launching mechanism, the flare-generated outflow must be exceptionally clean, launching an outflow with the Lorentz factor of at least few thousands, equation (9) assuming very low $\Gamma_{\rm w} \sim 30$. This is about an order of magnitude higher than that in GRBs. Wind models of the ejection are hopeless; the ejecta wind must be millions of times cleaner than the preceding magnetar wind (equation 34). Impulsive ejections have an advantage that they can reach terminal Lorentz factors $\sim \mu_0$, compared with $\mu_0^{1/3}$ for steady state.

Most importantly, we argue that in contrast to the hydrodynamic explosions (when the terminal Lorentz factor is determined either by ion loading or by pair freeze-out), the dynamics of the magnetic explosions is controlled by magnetic loading: the requirement of the conservation of the magnetic flux. Thus, in the case of magnetar explosions, the dynamics is drastically different from the fluid case; instead of shocks with Lorentz factors close to a million, the explosions reach force balance near the light cylinder and then either are advected with the wind as non-dissipative EM structure or propagate as EM pulses.

We also expect a type of magnetic loading to occur even for hydrodynamic explosions within a magnetosphere. If a hot fireball is created within a magnetosphere (not necessarily magnetically isolated), its expansion will lead to straightening out of a bundle of field lines. Thus, a large fraction of the energy of the fireball will be spent on distorting the magnetosphere. This will constitute a type of magnetic loading.

ACKNOWLEDGEMENTS

This work was supported by NASA grants 80NSSC17K0757 and 80NSSC20K0910 and by NSF grants 1903332 and 1908590. I would like to thank Andrei Beloborodov, Yuri Lyubarsky, and Lorenzo Sironi for discussions.

DATA AVAILABILITY

The data underlying this article will be shared on reasonable request to the corresponding author.

REFERENCES

Arons J., 1983, in Burns M. L., Harding A. K., Ramaty R., eds, AIP Conf. Proc. Vol. 101, Positron–Electron Pairs in Astrophysics. Am. Inst. Phys., New York, p. 163

Arons J., Scharlemann E. T., 1979, ApJ, 231, 854

Babul A.-N., Sironi L., 2020, MNRAS, 499, 2884

Barkov M. V., Luo Y., Lyutikov M., 2021, ApJ, 907, 109

Bellan P. M., 2000, in Bellan P. M., ed., Spheromaks: A Practical Application of Magnetohydrodynamic Dynamos and Plasma Self-organization. Imperial Coll. Press, London

Beloborodov A. M., 2017, ApJ, 843, L26

Beloborodov A. M., 2020, ApJ, 896, 142

Beloborodov A. M., Thompson C., 2007, ApJ, 657, 967

Blandford R. D., 2002, in Gilfanov M., Sunyeav R., Churazov E., eds, Proc. MPA/ESO/MPE/USM Joint Astron. Conf., Lighthouses of the Universe: The Most Luminous Celestial Objects and Their Use for Cosmology. Springer-Verlag, Berlin, p. 381

Blandford R. D., McKee C. F., 1976, Phys. Fluids, 19, 1130

Bochenek C. D., Ravi V., Belov K. V., Hallinan G., Kocz J., Kulkarni S. R., McKenna D. L., 2020, Nature, 587, 59

Cameron P. B. et al., 2005, Nature, 434, 1112

```
CHIME/FRB Collaboration, 2020, Nature, 587, 54
```

Coroniti F. V., 1990, ApJ, 349, 538

Farrugia C. J., Osherovich V. A., Burlaga L. F., 1995, J. Geophys. Res., 100, 12293

Gaensler B. M. et al., 2005, Nature, 434, 1104

Gallant Y. A., Arons J., 1994, ApJ, 435, 230

Goldreich P., Julian W. H., 1970, ApJ, 160, 971

Gourgouliatos K. N., Lynden-Bell D., 2008, MNRAS, 391, 268

Hibschman J. A., Arons J., 2001, ApJ, 560, 871

Hurley K. et al., 2005, Nature, 434, 1098

Israel G. L. et al., 2016, MNRAS, 457, 3448

Kennel C. F., Coroniti F. V., 1984, ApJ, 283, 694

Khangulyan D., Barkov M. V., Popov S. B., 2021, preprint (arXiv: 2106.09858)

Levinson A., 2010, ApJ, 720, 1490

Li C. K. et al., 2021, Nat. Astron., 5, 378

Lyubarsky Y. E., 2003, MNRAS, 345, 153

Lyubarsky Y., 2014, MNRAS, 442, L9

Lyubarsky Y., 2020, ApJ, 897, 1

Lyubarsky Y., 2021, Universe, 7, 56

Lyubarsky Y., Kirk J. G., 2001, ApJ, 547, 437

Lyutikov M., 2002a, Phys. Fluids, 14, 963

Lyutikov M., 2002b, ApJ, 580, L65

Lyutikov M., 2006a, APS April Meeting Abstracts, #X3.003

Lyutikov M., 2006b, New J. Phys., 8, 119

Lyutikov M., 2006c, MNRAS, 367, 1594

Lyutikov M., 2010, Phys. Rev. E, 82, 056305

Lyutikov M., 2011, MNRAS, 411, 422

Lyutikov M., 2017, Phys. Fluids, 29, 047101

Lyutikov M., 2021, preprint (arXiv:2102.07010)

Lyutikov M., Blandford R., 2003, preprint(astro-ph/0312347)

Lyutikov M., Camilo Jaramillo J., 2017, ApJ, 835, 206

Lyutikov M., Gourgouliatos K. N., 2011, Sol. Phys., 270, 537

Lyutikov M., Hadden S., 2012, Phys. Rev. E, 85, 026401

Lyutikov M., Popov S., 2020, preprint (arXiv:2005.05093)

Lyutikov M., Rafat M., 2019, preprint (arXiv:1901.03260)

Lyutikov M., Komissarov S. S., Porth O., 2016, MNRAS, 456, 286

Mehta R., Barkov M., Lyutikov M., 2021, MNRAS, 506, 6093

Mereghetti S. et al., 2020, ApJ, 898, L29

Metzger B. D., Berger E., Margalit B., 2017, ApJ, 841, 14

Metzger B. D., Margalit B., Sironi L., 2019, MNRAS, 485, 4091

Michel F. C., 1969, ApJ, 158, 727

Michel F. C., 1973, ApJ, 180, L133

Paczynski B., 1986, ApJ, 308, L43

Palmer D. M. et al., 2005, Nature, 434, 1107

Piran T., 2004, Rev. Mod. Phys., 76, 1143

Plotnikov I., Sironi L., 2019, MNRAS, 485, 3816

Porth O., Komissarov S. S., Keppens R., 2014, MNRAS, 438, 278

Porth O., Buehler R., Olmi B., Komissarov S., Lamberts A., Amato E., Yuan Y., Rudy A., 2017, Space Sci. Rev., 207, 137

Prendergast K. H., 2005, MNRAS, 359, 725

Rees M. J., Gunn J. E., 1974, MNRAS, 167, 1

Ridnaia A. et al., 2021, Nat. Astron., 5, 372

Sironi L., Spitkovsky A., 2009, ApJ, 698, 1523

Sironi L., Spitkovsky A., 2011, ApJ, 741, 39

This paper has been typeset from a TEX/IATEX file prepared by the author.